Thermodynamic study of solarized supercritical carbon dioxide cycle

Amit Kanaujiya

Department of Mechanical Engineering, Harcourt Butler Technical University, Kanpur (UP), India

Abstract: The supercritical carbon dioxide cycle run on the utilization of carbon dioxide uses emissions from fossil fuel-fired power plants. In this study, the supercritical carbon dioxide cycle is powered by solar energy using heliostat fields. The operating range of supercritical carbon dioxide cycle permits for the integration of low-temperature cycles for effective utilization of the heat remaining unutilized in it. This paper considers the supercritical carbon dioxide cycle for its energy analysis. It aims for the optimal utilization of heat available with the exhaust from the sCO_2 cycle. Results obtained based on parametric variation have been presented and analyzed here. At the turbine inlet pressure of 290 bar, the turbine inlet temperature of 700°C in sCO_2 cycle and cycle efficiency is obtained as 16.56 % and specific work output is 174.6 KJ/kg of sCO_2.

1. Introduction

Globallly the adverse impact of emissions demand for the power generation with minimum impact on the surroundings. The capture and use of carbon dioxide for power generation through the supercritical carbon dioxide (sCO_2) cycle is one of the attractive options. Supercritical carbon dioxide cycles operate on the Brayton cycle with carbon dioxide as a working fluid. Because of the constraint imposed by supercritical carbon dioxide, its exhaust carries a high amount of energy along with and can be harnessed for augmenting power output.

This section details some of the work done in this field. Turchi [1] pointed out the sCO_2 recompression Brayton cycle could offer the potential of equivalent or higher efficiency compared with supercritical or superheated steam cycles at temperature relevant for CSP applications. Seidel [2] compared efficiencies of several different sCO_2Brayton cycle layouts (including simple regeneration cycle, recompression cycle, precompression cycle, and split expansion cycle) as the alternative power blocks in CSP systems. It was found that the recompression cycle has the best thermal efficiency over a wide range of pressure ratios. Turchi et al. [3] also examined efficiencies of different sCO_2Brayton cycle layouts (including simple regeneration cycle, recompression cycle, partial cooling cycle, and intercooling cycle) with or without reheating for CSP applications. Neises et al. [4] performed a comparison of several different sCO_2Brayton cycle layouts with an emphasis on CSP applications. They compared the cycle efficiencies and the ability to integrate the thermal storage between the simple regeneration cycle, the recompression cycle, and the partial cooling cycle. Their results showed that the partial cooling cycle could offer higher efficiency than the recompression cycle until large quantities of conductance were modeled. The partial cooling cycle could also offer a larger temperature difference across the heat exchangers, allowing for more cost efficient thermal storage. Considering the transient nature of the solar resource, Iverson et al. [5] investigated the transient response of sCO_2Brayton cycles to fluctuating thermal input, respectively. Selection of a suitable cycle layout is an important topic for the application of sCO_2Brayton cycles in the SPT system. The literature review showed that the performances of different SCO_2Brayton cycles have been compared for solar power tower applications in the above studies. However, these studies were confined to investigate the sCO_2Brayton cycle separately. Few studies considered the unique characteristics of the solar receiver which have great effects on the performances of the whole system. It was normally assumed as a heat source that has similar heat outputs to those of the solar receiver. Recently, Padilla RV et al. [6] conducted a thermodynamic comparison of different sCO_2Brayton cycles (including simple Brayton cycle, simple regeneration cycle, precompression cycle, split expansion cycle, and the recompression cycle) integrated with SPT systems. In their study, both the solar receiver and the heliostat field were taken into account. They concluded that the recompression cycle offered the highest thermal efficiency. Behar O et al. [7] modeled the solar receiver as well as the power cycle, and performed aexergy analysis of several sCO_2Brayton cycles (including simple regeneration cycle, recompression cycle, partial cooling cycle, and intercooling cycle) integrated with SPT systems.

The literature review shows that there is a need for further analysis of the supercritical carbon dioxide cycle for better energy utilization in it. Thermodynamic analysis of the solar-powered sCO_2 cycle operating with the steam Rankine cycle and organic Rankine cycle is pertinent for studying the effect of different parameters on the performance of this combination.

2. System description of sCO_2 power system

Figure 1 is the schematic diagram of heliostat field-based solar-powered intercooler, reheat type sCO_2 cycle. The heliostat reflects solar radiation to the central reservoir carrying molten salt. In the present analysis, a mixture of $NaNO_3$(59.66%) and KNO_3 (40.44%) is used as the salt. The boiling temperature of the salt is 1400°C and the melting temperature is 310°C to 335°C, while the heliostat field offers temperature up to 1500°C [5]. Carbon dioxide enters the LPC at state 1 for being compressed to state2. For perfect intercooling, a heat exchanger is used between states 2 and 3 such that the temperature of state 3 is similar to that at state1.
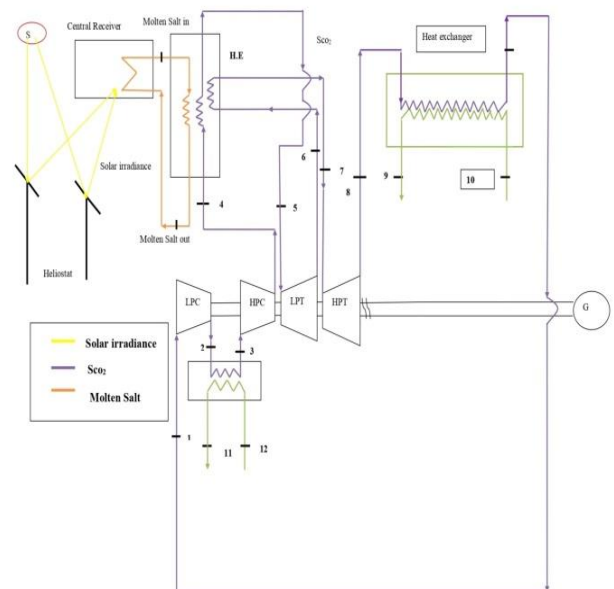
Fig. 1: Solarized combined sCO_2 cycle with intercooling and reheating arrangement in the sCO_2 cycle.

The compressed carbon dioxide then enters to HPC at state 3 for getting compressed up to the state 4.The compressed supercritical carbon dioxide then enters a molten salt heat exchanger, where it is

Corresponding Author,
E-mail address: amitme9026@gmail.com

heated using molten salt heat to state 5. The high pressure and high-temperature supercritical carbon dioxide enters at state 5 and then expanded in the HPT to state 6. Then the sCO_2 is reheated to state 7 in the molten salt heat exchanger and expanded in LPT to state 8.The expanded supercritical carbon dioxide is sent to the heat exchanger to utilization of remaining heat at state after heat exchanger the sCO_2 exit at state 1 and then enter to LPC.

3.Thermodynamic modeling

Thermodynamic modeling [14,13,7 and 15] of combined cycle components has been carried out based on the first law of thermodynamics. The following assumptions are considered for thermodynamic modeling.

1. All processes considered here are at a steady-state.
2. Direct Normal Irradiation is considered constant with a value of 1000 W/m².
3. No variation is considered in chemical energy of the material ,kinetic energy and potential energy
4. No pressure loss is considered.
5. Specific heat of supercritical CO_2 is taken from REFPROP 9.0
6. Inefficiency in compressor and turbine is considered through polytropic efficiency

3.1 Heliostat field and Central receiver

Energy balance for heliostat field is given by-

$Q_{max} = Q_{rec.} + Q_{lost}$ (1)

Where $Q_{max} = I. A_{he}$ (2)

Q_{max} is the total heat available in a given area (A_{he}) on incident solar radiation (I).

Due to some environmental factors (Irreversibility, conduction, convection, and radiation) a part of the heat is lost and remaining goes toreceiver (solar isolation). After considering energy losses, the energy efficiency of heliostat (η_h) is given by-

$\eta_h = Q_{rec}/Q_{max}$ (3)

Energy analysis for the receiver is given by-

$Q_{rec} = Q_{rec, abs} + Q_{rec, loss}$ (4)

Where $Q_{rec, abs}$ is the absorbed energy by receiver and $Q_{rec, loss}$ is energy lost in emission, reflection, convection and conduction. The efficiency of receiver is given as,

$\eta_{rec} = Q_{rec, abs}/ Q_{rec.}$ (5)

Specific heat of the molten salt in kJ/kg.K is given as,

$C_{p,sa} = 0.172T + 1443$[7]   (6)

The rate of molten salt absorbed heat can be expressed as:

$Q_{rec, abs} = m_{sa}.C_{p,sa}.(T_{sa,out} - T_{sa,in})$ (7)

$Q_{rec, loss} = Q_{loss,cond} + Q_{loss,conv} + Q_{loss,ems} + Q_{loss,ref}$ (8)

The receiver efficiency is given as-

$\eta_{rec} = Q_{rec, abs}/ Q_{rec.}$ (9)

$Q_{total} = Q_{max}.\eta_h.\eta_r$ (10)

3.2 sCO₂ cycle

The sCO_2 cycle is the Brayton cycle with supercritical carbon dioxide as its working fluid.

3.3 Compressor

Considering the polytropic efficiency of the compressor

$\eta_{poly-c} = (h_2 - h_1)/(h_{2'} - h_1)$ (11)

Work required for LPC is,

$w_{c1} = h_{2'} - h_1$ (12)

For perfect intercooling,

$T_3 = T_1$ (13)

Intercooling heat is,

$Q_{int} = m_s.(h_{2'} - h_3) = m_{int}.(h_{17} - h_{18})$ (14)

Between states 3 and 4,

$\eta_{poly-c} = (h_4 - h_3)/(h_{4'} - h_3)$ (15)

Work required for HPC is,

$w_{c2} = h_{4'} - h_3$ (16)

Total work required (KJ/kg) for the compressor is

$w_{cnet} = w_{c1} + w_{c2}$ (17)

3.4 Turbine

Considering polytropic efficiency,

$\eta_{poly-Turb} = (h_5 - h_{6'})/(h_5 - h_6)$ (18)

Work obtained from HPT is

$w_{T1} = h_5 - h_{6'}$ (19)

For perfect reheating,

$T_5 = T_7$ (20)

Between states 7 and 8,

$\eta_{poly-Turb} = (h_7 - h_{8'})/(h_7 - h_8)$ (21)

Work obtained from LPT is

$w_{T2} = h_7 - h_{8'}$ (22)

Total work available from turbines is

$w_{Tnet} = w_{T1} + w_{T2}$ (23)

Mass flow rate in sCO_2 cycle

$Q_{total} = m_s (h_5 - h_{4'}) + m_s(h_7 - h_{6'})$ (24)

work output of the topping cycle is given by-

$w_{s.net} = w_{Tnet} - w_{cnet}$ (25)

supercritical carbon dioxide cycle's energy efficiency is expressed by-

$\eta_s = (m_{s*} w_{s.net})/Q_{total}$ (26)

A computer program is written in C language for performance assessment with various input parameters using above equations.

4. Results and discussion

Results are obtained from the thermodynamic modeling and computer simulation of the solarized intercooled-reheat sCO_2 cycle for carbon-free power for the input parameters given in Table 1 and the property values from REFPROPand e-Thermo.

Table 1 Input parameters [3,4,11,12,13 and14]

| Parameters	Symbol, Unit	Value
Solar irradiation	I, W/m²	1000
Heliostat field area	A_{hf}, m²	10000
Heliostat efficiency	η_h, %	75
Receiver efficiency	η_{rec}, %	75
Polytropic efficiency of compressor	η_{poly_c}, %	89
Polytropic efficiency of turbine	η_{poly_turb}, %	93
Inlet temperature of compressor	T_1, ºC	32
Inlet pressure of compressor	P_1, bar	75
Inlet pressure of turbine	P_5, bar	250, 260, 270, 280, 290
Inlet temperature of turbine	T_5, ºC	600, 625, 650, 675, 700
Cycle pressure ratio	-	3.33,3.46,3.6,3.73, 3.86

(a)

(b)

(c)

(d)

(e)
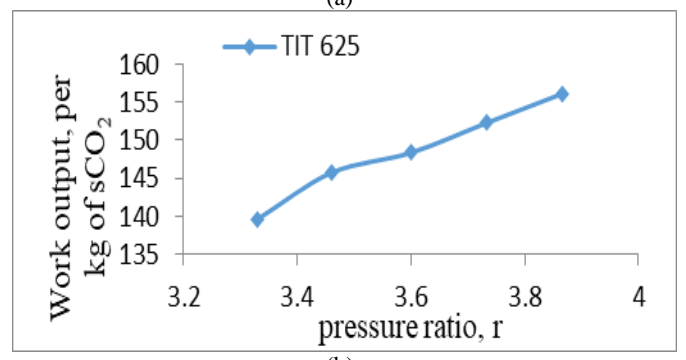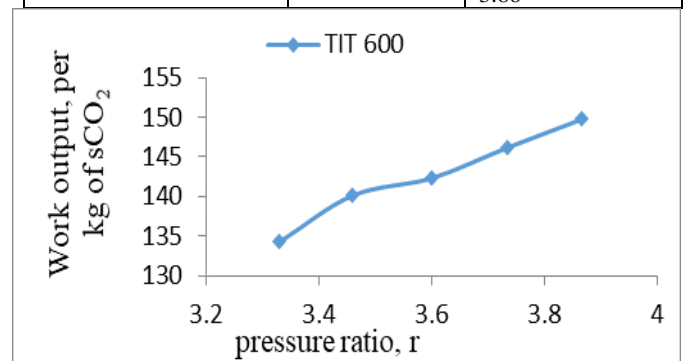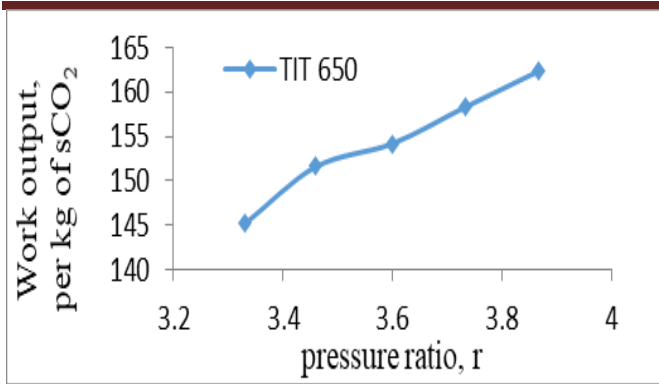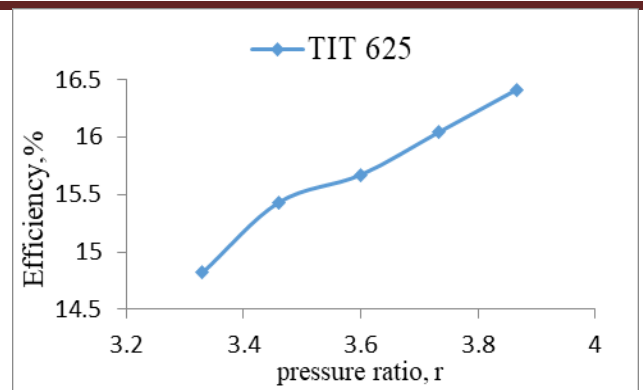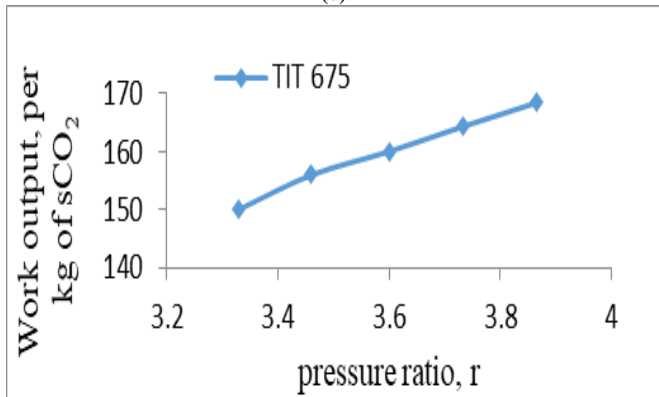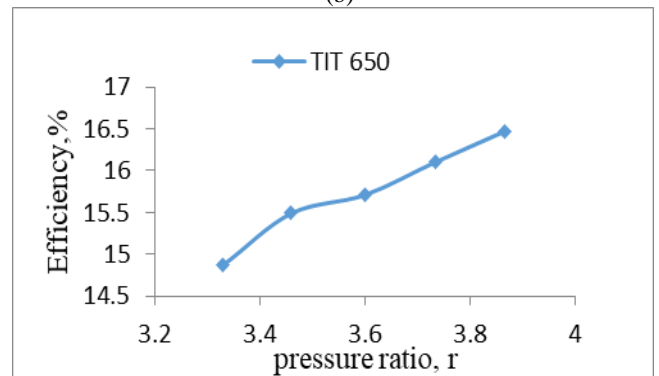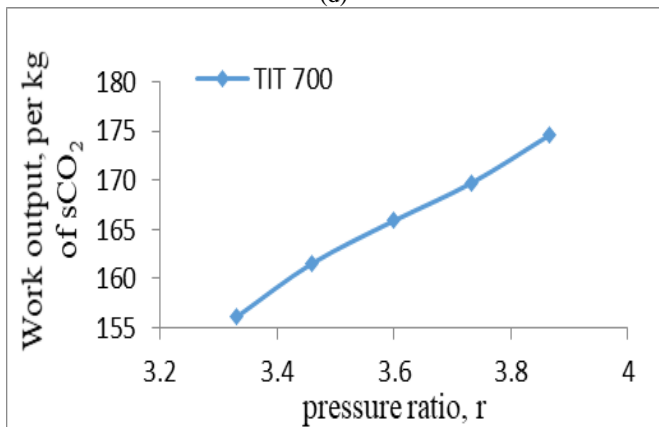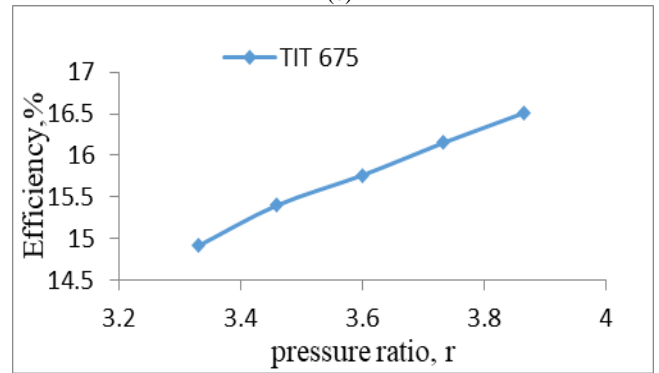
Fig. 2(a-e): Variation of specific work output with different TIT of sCO$_2$ cycle.

Figure 2 a-e show the variation of different work out put with cycle pressure ratio of sCO$_2$ cycle varying as 3.33,3.46,3.6,3.73,3.86.The work out put of sCO$_2$ cycle, is increases with an increase in cycle pressure ratio.The maximum work out putfor sCO$_2$ cycle is obtained as 174.6 kJat 260 bat and 700° C .

(a)

(b)

(c)

(d)
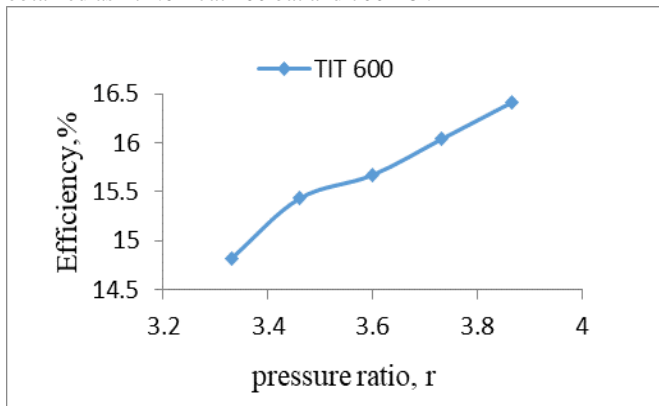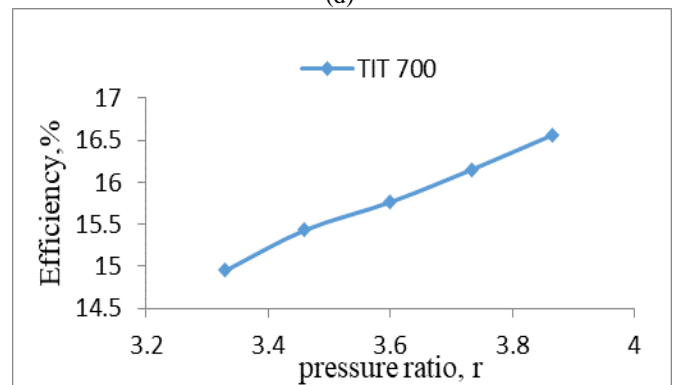
(e)

Fig. 3 (a-e): Variation of thermal efficiency with TIT of the sCO$_2$cycle for maximum pressures of sCO$_2$ cycle.

Figure 2 a-e show the variation of different efficiencies with cycle pressure ratio of sCO$_2$ cycle varying as 3.33,3.46,3.6,3.73,3.86. The efficiency of sCO$_2$ cycle,is increases with an increase in cycle pressure ratio.The maximum efficiency for sCO$_2$ cycle 16.56% at 290bar pressure, 700 ºC temperature at the inlet to sCO$_2$ turbine.

5. Conclusions

The following conclusions have been drawn from the thermodynamic study of solarized supercritical carbon dioxide cycle.

1. There is no emission of carbon as the supercritical carbon dioxide is the working fluid in the sCO_2 cycle, so it is an eco-friendly cycle.
2. There is a limitation of the sCO_2 cycle as the limiting pressure and temperature values are 73.773bar and 31.13°C for being in the supercritical stage.
3. In the sCO_2 the maximum overall thermal efficiency is 16.56% and the specific work output is 174.6 kJ per kg of sCO_2.

Acknowledgement

Nomenclature

1, 2, 3….12	Cycle states as shown in the schematic diagram
$T_{sa,in}$	Molten salt inlet temperature to the central receiver
I	Solar radiation
A_{he}	Heliostat Area, m^2
av	Availability
$T_{sa,out}$	Molten salt outlet temperature from central receiver
Cond.	Condenser
CPR	Cycle Pressure Ratio
CSP	Concentrated solar power
E	Energy
G	Generator
h	Enthalpy
HPC	High-Pressure compressor
LPC	Low-Pressure compressor
HPT	High-Pressure turbine
LPT	Low-Pressure turbine
LPST	Low-pressure steam turbine
TIT	Turbine inlet temperature
m	Mass
P	Pressure
p	Pump
Q	Heat
rec	Receiver
s	Entropy
sCO_2	Supercritical carbon-di-oxide
T	Temperature
Turb	Turbine
MSHE	Molten salt heat exchanger
w	Work per unit mass
W	Work
η	Efficiency
Subscripts	
air	Air
abs	Heat absorbed by molten salt
amb.	Ambient
c	Compressor
T	Turbine
C_p	Specific heat
cond.	Condenser
h_e	Heliostat
isen	Isentropic
rec.	Receiver
int.	Intercooling
loss	Heat loss
m_s	A mass flow rate of supercritical carbon dioxide
poly_c	Polytropic for compressor
poly_turb	Polytropic for turbine
st.	Steam
sa	Molten salt
s.	Supercritical carbon dioxide
int.	Inter cooling

References

[1] CS Turchi, Z Ma, J Dyreby. Supercritical CO2 for application in concentrating solar power systems. In: S-CO2 Power Cycle Symposium, RPI, Troy, NY, 4, 2009.

[2] W Seidel. Model development and annual simulation of the supercritical carbon dioxide Brayton cycle for concentrating solar power applications Master thesis. The University of Wisconsin-Madison. 2014.

[3] CS Turchi,Z Ma, TW Neises. Thermodynamic study of advanced supercritical carbon dioxide power cycle for concentrating solar power. J Sol Energy Eng 135, 2013,041007.

[4] T Neises, C Turchi. A comparison of supercritical carbon dioxide power cycle configurations with an emphasis on CSP applications. Energy Procedia 2014;49:1187–96.

[5] BD Iverson, TM Conboy, JJ Pasch, AM Kruizenga Supercritical CO_2 Brayton cycles for solar-thermal energy. Appled Energy111, 2013, 957–70.

[6] RV Padilla, YC SooToo, R Benito. Exergetic analysis of supercritical CO2 Brayton cycles integrated with solar central receivers. Appled Energy148, 2015, 348–65.

[7] O Behar, A Khellaf, K Mohammedi. A review of studies on central receiver solar thermal power plants. Renew Sustain Energy Rev 23, 2013, 12–39.

[8] T Neises, C Turchi. A comparison of supercritical carbon dioxide power cycle configurations with an emphasis on CSP applications. Energy Procedia 49:1187 – 1196.

[9] S Shaaban. Analysis of an integrated solar combined cycle with steam and organic Rankine cycles as bottoming cycles. Energy Conversion and Management 126, 2016,1003–1012.

[10] S Jatin, O Singh. Thermodynamic analysis of solar-powered triple combined Brayton. Rankine and organic Rankine cycle for carbon-free power. Renewable energy 139, 2019, 765-780.

[11] S Shaaban Analysis of an integrated solar combined cycle with steam and organic Rankine cycles as bottoming cycles. Energy conversion and management 126, 2016, 1003-12.

[12] SS Mohamed, F Mehmet, U Faruk. Thermodynamic analysis of parabolic trough and heliostat field solar collectors integrated with a Rankine cycle for cogeneration of electricity and heat. Solar field 136, 2016, 183-196.

[13] M Rabbani, TAH Ratlamwala, I Dincer. Transient Energy and Exergy analyses of a Solar Based Integrated System. Journal of Solar Energy Engineering 137, 2015.

[14] D Thoranis, K Tanongkiat, T